

Uncertainties in Estimating Hadronic Production of the Meson B_c and Comparisons between TEVATRON and LHC

Chao-Hsi Chang^{1,2} * and Xing-Gang Wu^{2†}

¹*CCAST (World Laboratory), P.O.Box 8730, Beijing 100080, China.*[‡]

²*Institute of Theoretical Physics, Chinese Academy of Sciences,
P.O.Box 2735, Beijing 100080, China.*

Abstract

The most estimates of hadronic production of the meson B_c in literature are based on perturbative QCD (pQCD) factorization at the lowest order (the ‘complete calculation approach’) and on the mechanism being dominant by the hard subprocess $gg \rightarrow B_c(B_c^*) + b + \bar{c}$, here we quantitatively studied the uncertainties in the estimates, which may be attributed to certain variations of the relevant parameters to the potential model, various versions of the parton distribution functions, especially, those relevant to α_s -running and the characteristic energy scale of the process where the QCD factorization is made etc. To be references, possible consequences from the kinematics cuts which match the real detectors at TEVATRON and LHC were also discussed. In the meantime we also pointed out that at TEVATRON due to the collision c.m. energy increasing, the total cross-section of the B_c production with proper kinematics cuts increase about 20% from RUN-I to RUN-II. From the quantitative studies, one may also see the fact that the experimental studies of the meson B_c at TEVATRON and at LHC will be complimentary and simulative.

PACS numbers: 12.38.Bx, 13.85.Ni, 14.40.Nd, 14.40.Lb.

Keywords: B_c meson, inclusive hadronic production, uncertainties.

* email: zhangzx@itp.ac.cn

† email: xgwu@itp.ac.cn

‡ Not correspondence address.

I. INTRODUCTION

B_c -physics is attracting more and more interests recently due to its experimental progresses (experimental discovery)[1] and theoretical ones [2, 3, 5, 6, 7, 8, 9, 10, 11, 12, 13, 14, 15, 16, 17]. Since only at high energy hadronic colliders can one collect numerous enough B_c mesons [2, 3, 5, 6, 7, 8, 9] and considering various usages for experimental further feasibility studies on relevant topics, recently in Ref.[18] a computer generator, BCVEGPY, for hadronic production of B_c is completed, which is a Fortran program package to be implemented in PYTHIA[19].

The hadronic production of the meson B_c and B_c^* [25] has been estimated by the authors of Ref.[6, 10] with the fragmentation approach, and the authors of Refs.[7, 8, 9] with the so-called ‘complete approach’ i.e. completely to compute the production through the dominant ‘hard’ subprocess of perturbative QCD (pQCD) $gg \rightarrow B_c(B_c^*) + \bar{c} + b$ at the lowest order (LO) (α_s^4). Note here: $m_b \gg m_c \gg \Lambda_{QCD}$, so apart from the binding factor that a pair of quarks c and \bar{b} bind to the double heavy meson B_c , the subprocess essentially is a ‘hard’ one in the sense of pQCD[7, 8, 9]. The two approaches both are based on the QCD factorization of a hard subprocess and the non-perturbative factors. Within theoretical uncertainties the two approaches agree essentially, especially, when the fragmentation approach additionally takes into account the contribution from gluon fragmentation[10]. The fragmentation approach is comparatively simple and can reach to leading logarithm order (LLO) accuracy of pQCD, but is satisfied only in the case if one is interested only in the produced $B_c(B_c^*)$ itself. The complete calculation approach has a great advantage, that it retains the information about the \bar{c} and b quark (jets) associated with the B_c meson in the production. From the experimental point of view this is a more relevant case. Therefore, BCVEGPY adopted the complete calculation approach (full pQCD complete calculation at the lowest order α_s^4) to the subprocess $gg \rightarrow B_c(B_c^*) + \bar{c} + b$ for the hadronic production program of B_c . In fact, according to pQCD, there are various production mechanisms, such as those via a quark pair annihilation subprocess, $q\bar{q} \rightarrow B_c(B_c^*) + \bar{c} + b$ and the color octet components of B_c . Since the ‘luminosity’ (structure function’s product) of gluons is much higher than that of quarks in pp collision (LHC) and in $p\bar{p}$ collision (TEVTRON), furthermore, there is an S -channel suppression factor for the annihilation of the quark-antiquark pair mechanism due to the virtual gluon propagator of the annihilation, the contribution from the annihilation

mechanism is negligible to compare with the dominant (concerning) one. The component of the color octet is small and for the ‘octet component mechanism’ there is no such an enhancement as in the hadronic production of $J/\psi, \psi'$, the contributions from color octet components of B_c in the production are ignorable at all. Therefore, the calculations in Refs.[6, 8, 9, 10] are neglected the contribution from the quark pair mechanism and the ‘color octet mechanism’. The program BCVEGPY ignored the mechanisms too.

It is known that the estimated hadronic production of the meson B_c in literature Refs.[6, 8, 9, 10] is in consistecy only within theoretical uncertainties (sometimes the differences of the results can be so great almost as one magnitude), and furthermore concerning the fact that RUN-II of TEVTRON is carrying on now and LHC is under constructing, various experimental feasibility studies of B_c meson are in progress, thus quantitatively to know the uncertainties in the estimates of the B_c production is interesting for experimental feasibility studies and for theoretically going beyond LO. Thus this paper is devoted to studying the uncertainties quantitatively.

The newly developed generator BCVEGPY[18] with various options to compute the production is well tested by carefully comparing obtained results with those of earlier references Ref.[7], and it may be applied to simulating generation of the B_c events stochastically (Monte Carlo simulation). Thus BCVEGPY is a suitable tool to study the uncertainties, so we would adopt the tool in the paper.

Although quite a lot of uncertainties can be fixed (suppressed) when next order of pQCD calculation is achieved, since a complete pQCD calculation on the production to the next order is too complicated, thus here we would restrict ourselves to examine the uncertainties only to the lowest order pQCD. We would use BCVEGPY to carry out the precise computations through variation in ‘reasonable regions’ of the factors so as to see the consequences of the variation clearly. Namely in the paper the uncertainties of the estimates for the approach of complete α_s^4 calculating the hard subprocess $gg \rightarrow B_c(B_c^*) + b + \bar{c}$ are focused. The uncertainties examined in the paper would contain those come from various versions of the parton distribution functions given by various groups, and the variation of the parameters in the estimates relevant to the potential model, α_s -running, the characteristic energy scale of the process where the pQCD factorization are carried out, etc. Possible and naive kinematics cuts to ‘match’ the detectors at TEVATRON and at LHC are also discussed. As a result of the study, we also showed precisely that the experimental studies of B_c will

be complimentary and simulative each other for TEVATRON RUN-II and at LHC. As for the special interesting topic to study $B_s - \bar{B}_s$ mixing and CP violation in the B_s meson decays at high energy hadronic colliders only through the B_s mesons which are produced and tagged by the decays of B_c [26], since at LHC, with a higher luminosity for the collisions and a higher cross section of the production than that at TEVATRON, numerous B_c as 10^{8-9} events per year, higher than those at TEVATRON by $3 \sim 4$ order, may be obtained, so such an interesting studies of B_s meson may be more practical at LHC than at TEVATRON in RUN-II.

The paper is organized: following Introduction, in Section II we present the studies of the various uncertainties in the estimates of the hadronic production of the meson B_c . In Section III, we present the studies of the consequences of various kinematics cuts which dictate the situation of the detectors at TAVATRON and at LHC. In the meantime we compute the changes precisely when the collision energy increases as that from RUN-I to RUN-II. In the last section, we make a short summary of the present study of this paper.

II. THE UNCERTAINTIES IN ESTIMATES

At high energy, the gluon-gluon fusion process $gg \rightarrow B_c(B_c^*) + b + \bar{c}$ is the dominant source of hadronic B_c production[27]. In order to fucus the dominant mechanism, the uncertainties of hadronic production of the meson $B_c(B_c^*)$ from the other mechanisms, such as pointed out in Introduction, are omitted in the paper. Based on the factorization of perturbative QCD (pQCD), the hard subprocess and the non-pertibative factor are the key parts of the production. In the sub-sections below, we discuss the uncertainty factors of the non-perturbative one and those of the hard subprocess.

A. Uncertainties Relevant to Quark Masses and Potential Model Parameters

In the leading order approximation for the production, the decay constant f_{B_c} of the meson B_c appears in the amplitude, so the production cross sections are proportional to it squared, and it can be related to the wave function at origin of the potential model through the following formula,

$$f_{B_c}^2 = \frac{12|\Psi_{[1S]}(0)|^2}{M_{B_c}}, \quad (1)$$

(It has no relation to spin of $B_c[1^1S_0]$ and $B_c^*[1^3S_1]$ because the effects from spin splitting are of high order) and where M is the $B_c(B_c^*)$ meson's mass (the binding system $(c\bar{b})$ at $[1S]$ level). Though the value of f_{B_c} can be determined from the potential model within a region, so a uncertainty comes from it. Since the total cross section is proportional to the square of the decay constant f_{B_c} , so the value of f_{B_c} affects the total cross section as a whole factor explicitly. It is for this reason, in the paper, that we would not study the uncertainty caused by the decay constant f_{B_c} further. Thus for preciseness and not losing convenience, throughout the paper we take the value of f_{B_c} to be 0.480GeV for $c\bar{b}(\bar{c}b)$ in $[1S]$ level; and 0.320GeV for $c\bar{b}(\bar{c}b)$ in $[2S]$ level[11]. Thus the hadronic cross sections for $[1S]$ level will roughly be 2.25 times as large as those of the $[2S]$ level.

Except the decay constant f_{B_c} , the values of the effective quark masses (c and b quarks' masses) that have been involved in the process also will generate a sensible uncertainties to the hadronic production of $B_c(B_c^*)$. In the following, we take the c quark mass as a basic input to show the uncertainty from the c quark effective mass how to affect the hadronic production of $B_c(B_c^*)$ quantitatively. For the c quark effective mass, we take it's value in the range of

$$1.4GeV \leq m_c \leq 1.6GeV, \quad (2)$$

which covers the frequently used values in the literature. And for the mass of $B_c(B_c^*)$, we take the central value of the experimental results($M_{B_c}^{exp} = 6.4 \pm 0.39 \pm 0.315\text{GeV}$ [1]), i.e., $M_{B_c^*} \simeq M_{B_c} = 6.4\text{GeV}$. Under the leading order approximation, the relative momentum between the constitute quarks is ignored, in addition, to satisfy the demand of the gauge invariance the b quark's mass is fixed by the relation, $m_b = M_{B_c}(M_{B_c^*}) - m_c$.

In TABLE I, we give the total cross-sections for the hadronic production of $B_c[1^1S_0]$ and $B_c^*[1^3S_1]$ at TEVATRON and at LHC. As will be shown in the following sections, since there are the other factors which may bring uncertainties into the production, for clarity, in TABLE I, the parton distributions are fixed at leading order i.e. the version CTEQ5L[21], while the strong coupling α_s is running at the leading order and the characteristic energy scale of the process (where the factorization is taken) is taken as $Q^2 = \bar{s}/4$ where \bar{s} is the c.m. energy squared of the subprocess.

From the TABLE I, one may observe that the quark masses affect the total hadronic cross section to a degree, such as when the value changes by 0.1GeV, then the total cross section change about 10% – 20%, i.e., the total cross section decrease with increasing of the c mass

TABLE I: The total cross section (in unit nb) for hadronic production of $B_c[1^1S_0]$ and $B_c^*[1^3S_1]$ mesons with various values of c quark mass. The gluon distribution function: CTEQ5L, the characteristic energy scale: $Q^2 = \bar{s}/4$ and the running α_s in leading order(LO). The number following each value in the parenthesis means the statistics error due to Monte Carlo numerical integration.

-	TEVATRON			LHC		
$m_c(GeV)$	1.4	1.5	1.6	1.4	1.5	1.6
$\sigma_{B_c}(nb)$	3.714(4)	3.213(3)	2.811(2)	58.49(8)	51.33(6)	44.53(5)
$\sigma_{B_c^*}(nb)$	9.28(1)	7.72(1)	6.503(3)	151.3(3)	126.5(2)	107.1(2)

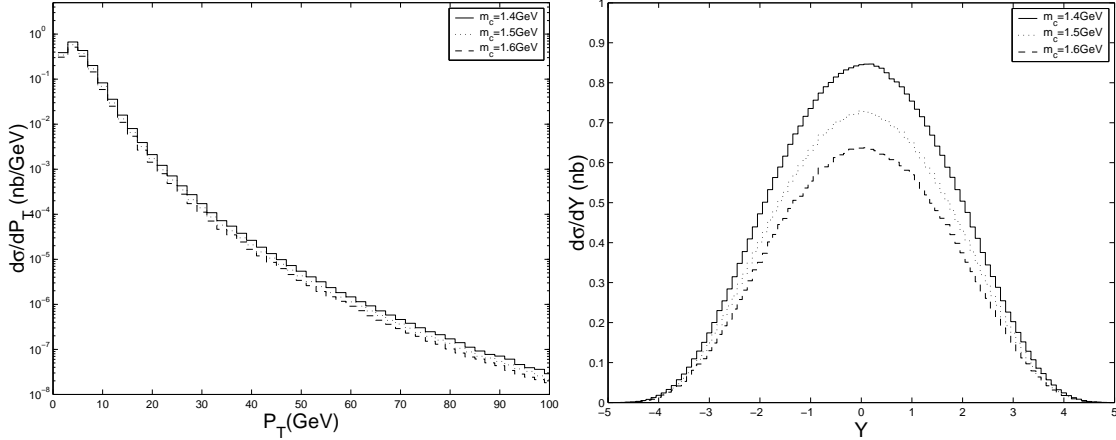


FIG. 1: The differential transverse-momentum P_T and rapidity Y distributions of B_c with different c quark mass at TEVATRON. The solid, dotted and dashed lines here stand for $m_c = 1.4, 1.5, 1.6$ GeV respectively.

(and decreasing of the b quark mass). To show this more clearly, we draw the differential distributions of the transverse momentum P_T and rapidity Y of $B_c(B_c^*)$ in FIGs.1,2,3,4 respectively. In FIGs.1,2, the results for the pseudoscalar B_c at TEVATRON and at LHC are shown, while in FIGs.3,4, the results for the vector B_c^* at TEVATRON and at LHC are shown.

Having known the uncertainties from quark masses, in the studies to focus on the others in the $B_c(B_c^*)$ meson hadronic production, later on we will take a fixed value of the mass

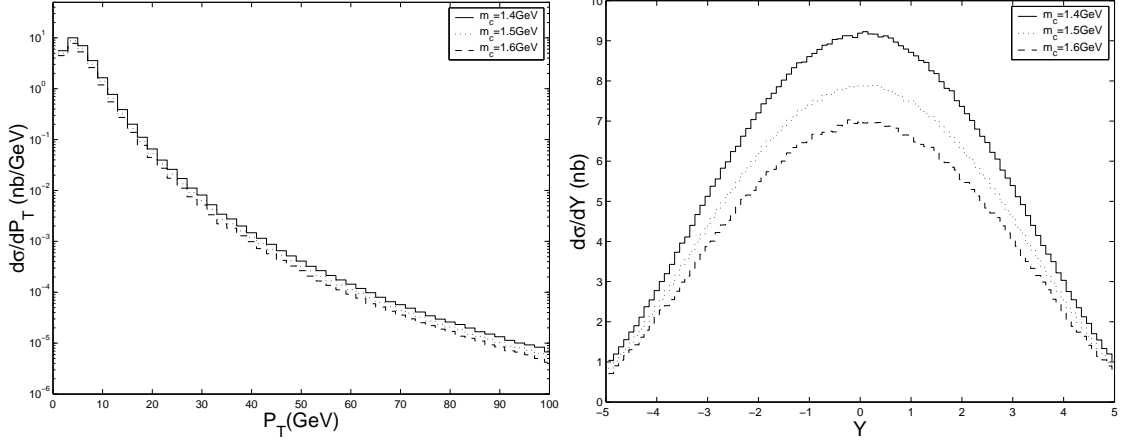


FIG. 2: The differential transverse-momentum P_T and rapidity Y distributions of B_c with different c quark mass at LHC. The solid, dotted and dashed lines stand for $m_c = 1.4, 1.5, 1.6$ GeV respectively.

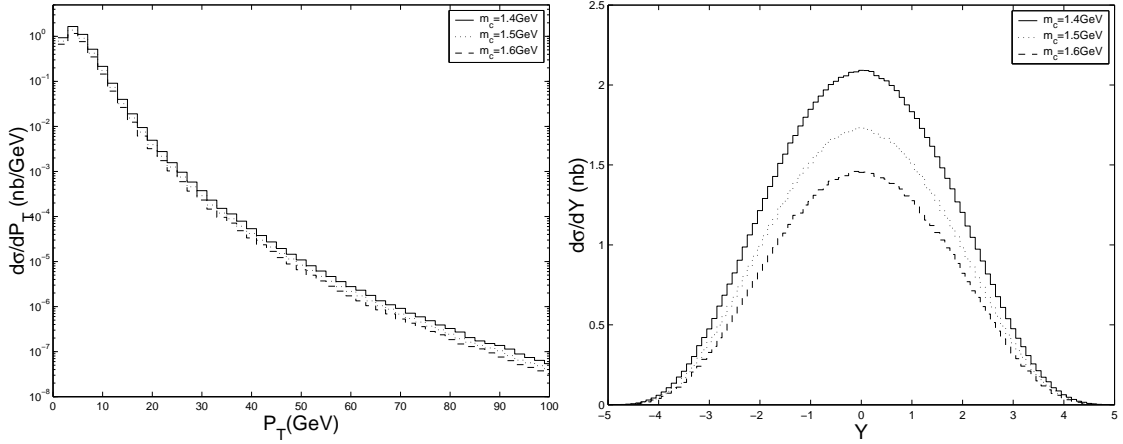


FIG. 3: The differential transverse-momentum P_T and rapidity Y distributions of B_c^* with different c quark mass at TEVATRON. The solid, dotted and dashed lines stand for $m_c = 1.4, 1.5, 1.6$ GeV respectively.

for c -quark and b -quark. For $[1S]$ energy level we take $M_{B_c[1S]} = 6.4$ GeV (central value of the experimental observation[1]), $m_c^{eff} = 1.5$ GeV and $m_b^{eff} = 4.9$ GeV; while for B_c^{**} ($[2S]$ energy level) we take $M_{B_c^{**}[2S]} \simeq 6.9$ GeV (from the potential model), $m_c^{eff} = 1.8$ GeV and $m_b^{eff} = 5.1$ GeV[11].

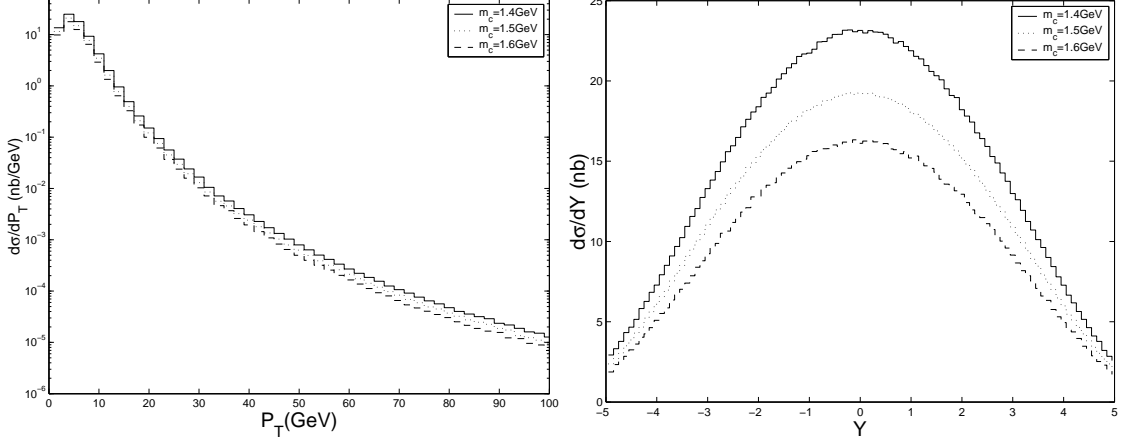


FIG. 4: The differential transverse-momentum P_T and rapidity Y distributions of B_c^* with different c quark mass at LHC. The solid, dotted and dashed lines stand for $m_c = 1.4, 1.5, 1.6$ GeV respectively.

B. Uncertainties Relevant to QCD Factorization and Parton Distribution

The ‘completed’ calculations on the hadronic production of the $B_c(B_c^*)$ meson are based on the factorization:

$$\begin{aligned}
 d\sigma &= \sum_{ij} \int dx_1 \int dx_2 F_{H_1(P_1)}^i(x_1, \mu_F^2) \times F_{H_2(P_2)}^j(x_2, \mu_F^2) d\hat{\sigma}_{ij \rightarrow B_c b \bar{c}}(P_1, P_2, x_1, x_2, \mu_F^2), \\
 &\simeq \sum_{ij} \int dx_1 \int dx_2 F_{H_1(P_1)}^i(x_1, \mu_F^2, \mu_R^2) \times F_{H_2(P_2)}^j(x_2, \mu_F^2, \mu_R^2) \cdot \sum_{m=0}^n \left[\alpha_s^4(\mu_R^2) \right. \\
 &\quad \cdot d\hat{\sigma}_{ij \rightarrow B_c b \bar{c}}^{(m)}(P_1, P_2, x_1, x_2, \frac{Q^2}{\mu_F^2}, \frac{Q^2}{\mu_R^2}) \left. \right]
 \end{aligned} \tag{3}$$

with a suitable number n (the order of the calculation), where $F_{H_1(P_1)}^i(x_1, \mu_F^2)$ and $F_{H_2(P_2)}^j(x_2, \mu_F^2)$ are the structure functions of incoming hadrons H_1 (momentum P_1) and H_2 (momentum P_2) for parton i (with the momentum fraction x_1) and parton j (with the momentum fraction x_2) respectively; μ_F is the energy scale where the factorization for non-perturbative factor (the structure functions) and perturbative one are carried out; $d\hat{\sigma}_{ij \rightarrow B_c b \bar{c}}(P_1, P_2, x_1, x_2, \mu_F^2)$ is the differential cross-section of the hard subprocess; μ_R is the energy scale where the renormalization is carried out; $d\hat{\sigma}_{ij \rightarrow B_c b \bar{c}}^{(m)}(P_1, P_2, x_1, x_2, \frac{Q^2}{\mu_F^2}, \frac{Q^2}{\mu_R^2})$ is the differential cross-section of the hard subprocess at the order higher than the lowest one by m order and Q^2 is the characteristic energy squared.

Most of the estimates on the production is at leading (the lowest) order (LO) of pQCD

i.e. $n = 0$ is set in Eq.(3). While for simplicity, the energy scale (squared) μ_F^2 where the factorization is carried out may be further taken either to be equal to the energy scale of renormalization μ_R^2 or to be equal to Q^2 etc in principal, i.e. even though there are still various choices. In practice to pursue an accurate result at the lowest order, how to choose μ_F and μ_R properly becomes important and cannot be solved by the leading order calculations themselves. If the calculations at higher orders (say $n = 1$ NLO and $n = 2$ NNLO for instance) are available the problem can be solved (suppressed) quite a lot theoretically. Whereas, as pointed in Introduction, for the production of the meson B_c the calculations is very complicated, that at leading order for the subprocess there are 36 Feynman diagrams with two massive fermions in final state needed to compute precisely, so the next order calculations (NLO, NNLO) on the subprocess (much more complicated) are not available so far. Thus at this moment one has to apply the leading order formulation to estimate the production, and here we study the uncertainties of the estimates by making the possible choices with pQCD experiences from the other processes about those of the lowest order and higher order ones being guidance. Namely here with pQCD experiences from the other processes being guidance, we choose possible μ_F, μ_R and Q^2 of Eq.(3) etc, and compute the observables quantitatively, then the different results obtained by the different choices, being considered as the uncertainties of the LO estimates, are shown precisely.

In fact, reviewing the choices of the literature, here we choose some of typical ones only to compute the various cross sections of the B_c hadronic production.

The parton (gluon) distributions for the production, $F_{H_1(P_1)}^i(x_1, \mu_F^2)$ and $F_{H_2(P_2)}^j(x_2, \mu_F^2)$ with $i, j = gluon$; $H_1 = proton, H_2 = proton$ for LHC; $H_1 = proton, H_2 = anti - proton$ for TEVATRON; in Eq.(3), are customarily interpreted as probability densities in finding a parton carrying a momentum fraction between x_i and $x_i + dx_i$ in hadrons. The distribution functions are factorized out from the whole production process by pQCD as non-perturbative factors at energy scale μ_F^2 . Note that usually the factorization is carried out at the characteristic energy scale of the hard subprocess Q^2 i.e. $\mu_F^2 = Q^2$ so later on we use Q^2 and μ_F^2 on ‘equal foot’. Being essentially non-perturbative so un-calculable, they can only be achieved through global fit experimental data within the pQCD framework (pQCD evolution with characteristic momentum Q^2 being taken into account). There are several groups (CTEQ, GRV, MRS and etc.) who are devoted to achieve accurate parton distributions. Some of them have programmed their results, which can be conveniently obtained from WWW, and

develop the programmes with time being to issue various versions so as to catch up with the newly obtained experiment data in the global fit. Therefore due to the data being adopted and the way to treat experimental errors, the choice of renormalization schemes and the assumptions on the initialization of some distributions etc, the parton distributions are different from various issues (various versions and obtained by various group). In the present study, we consider three gluon distributions, which are achieved by three groups CTEQ, GRV and MRS, quantitatively and with them to compute the cross sections so as to show the uncertainties from the parton distributions (in literature various parton distributions were used).

To show the differences of the parton distributions, we draw the curves obtained by CTEQ, GRV and MRS in FIG. 5. The curves in the figure are obtained just from straightforward calculations at two characteristic energy scales $Q^2 = 10^2 GeV^2$ and $Q^2 = 10^5 GeV^2$ with the programmes obtained from the web addresses[28]. From the figure, one may see that the gluon distributions are quite coincide each other in most regions of x , but in some particular place (the small x region) the differences of them are visible.

As stated in the introduction, since the B_c meson production is dominant by the subprocess $gg \rightarrow B_c(B_c^*) + \bar{c} + b$ and the generator BCVEGPY is programmed based on the dominant subprocess to perturbative QCD (pQCD) at leading order, thus to be self-consistent for the comparisons, in most case without precise indication, in our studies we choose the gluon distributions also of leading order, i.e., the three CTEQ5L[21], GRV98L[23] and MSRT2001L[24] ('L'-version). Furthermore for a more general comparison and in order to have some knowledge on the higher order corrections, a few times for the studies, we also try to choose the two NLO versions of the gluon distributions CTEQ3M[22] and CTEQ5M[21] (the next to leading order 'M'-version).

Running of the strong coupling constant α_s may be independent on the factorization in some degree and it determines the evolution of the parton distributions and the hard subprocess essentially. According to renormalization group (RG), it may cover the quantum correction effects of pQCD in a simple process if the energy scale is chosen properly. Therefore the problem appears how to make the estimates at LO more accurate just by determining α_s running and the characteristic energy scale Q^2 for the hard subprocess and for the parton distribution functions. In fact, the problem may be solved partly by the proving pQCD factorization up to higher orders in principal.

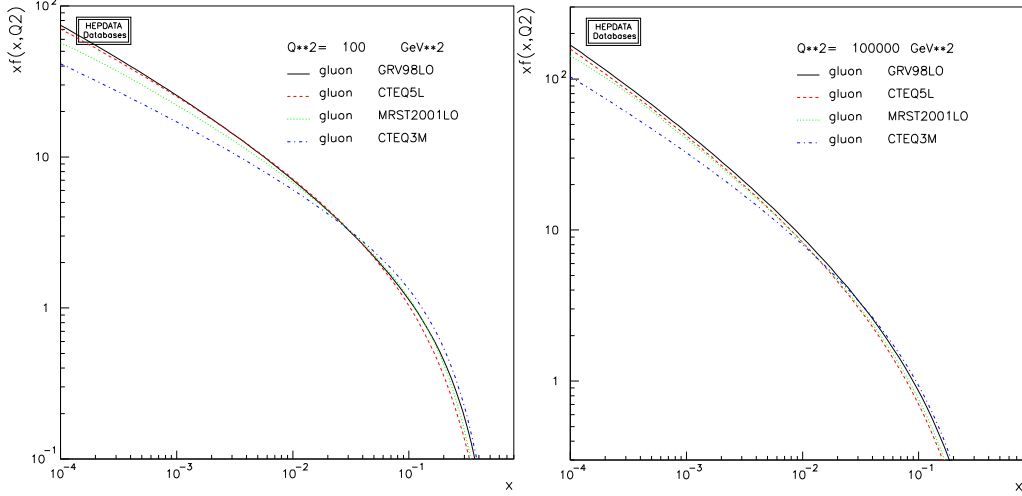


FIG. 5: The different gluon distributions $xf(x, Q^2)$ (MSRT2001L, GRV98L, CTEQ5L and CTEQ3M) at two characteristic energy scales: $Q^2 = 10^2 GeV^2$, $Q^2 = 10^5 GeV^2$. Here the solid, dashed, dotted and dash-dotted lines stand for the gluon distributions GRV98L, CTEQ5L, MSRT2001L and CTEQ3M respectively.

According to the factorization at LO, α_s running should be leading logarithm one (LLO) and all of the energy scale Q^2 appearing in the calculation should take the same value as the characteristic energy scale of the hard subprocess. Whereas in the literature there are quite different treatments on the problem with certain arguments but without proof. Here following the authors in the literature, we try some typical treatments to see the uncertainties from these sources. To achieve a satisfied accuracy in the estimates at LO, it is crucial to choose the factorized energy scale(s) and how to relate to the characteristic energy scale of the hard subprocess Q^2 . However, due to the fact that in the production of $B_c(B_c^*)$, there are several energy scales in the process, such as $Q^2 = m_c^2$, $Q^2 = m_b^2$, transverse momentum $Q^2 = p_T^2$ of B_c and center mass system energy of the subprocess $Q^2 = \frac{1}{4}\bar{s}$ (\bar{s} is the CM energy of the subprocess) etc. in principal (because $Q^2 \gg \Lambda_{QCD}^2$), therefore the various possible choices of them were made in the literature.

In the three types of leading order gluon distributions CTEQ5L, GRV98L and MSRT2001L, the QCD evolution effects have already been included. Whereas to study the uncertainties, we tried to give up the exact LO request such as to let α_s run as LLO and let the energy scale appearing in the calculation be different from the characteristic energy scale Q^2 of the hard subprocess. To be precise for the uncertainty study, the energy scale

for α_s running (even LLO) is taken as the same as Q^2 that in subprocess $gg \rightarrow B_c + b + \bar{c}$. In fact, in the B_c hadronic production there are two factors which may be factorized in principal, i.e., one of which is the non-perturbative factors of the parton distributions and the other one is the bound state factor in the subprocess $gg \rightarrow B_c + b + \bar{c}$. Thus besides α_s running (including the choice of the value Λ_{QCD} etc), for the characteristic energy scales of the subprocess there is arbitrariness within a certain reasonable ranges such as $Q^2 : 4m_c^2 \Rightarrow M_{B_c T}^2(\frac{1}{4}\bar{s})$ where $M_{B_c T}^2 \equiv P_T^2 + M^2$ is the so-called ‘transverse mass’ of the meson B_c ; \bar{s} is the c.m. (center mass) energy of the subprocess. In Refs.[7, 8, 20], some of suggestions on the value of Λ_{QCD} and the characteristic energy scale Q^2 for the subprocess are provided. Here considering the different consequences due to the different choices about α_s running and the characteristic energy scales, we make the typical choices on α_s running and the characteristic energy scale(s) etc to compute various observables of the production and to show the uncertainties (systematic comparison on the differences) quantitatively.

In the running coupling constant α_s for the hard sub-processes of generating $B_c(B_c^*)$ meson and for the parton distributions, the value of Λ_{QCD} , which is a measurement of the momentum, is scheme dependent, to be precise throughout the study we use the modified minimal subtraction one: $\Lambda_{\overline{MS}}$. The leading order (LO) running coupling constant α_s has the form,

$$\alpha_s(Q^2) = \frac{12\pi}{(33 - 2n_f) \ln(Q^2/\Lambda_{\overline{MS}}^2)}, \quad (4)$$

where, n_f is the number of the active quark flavors under the particular energy scale Q^2 . The next to leading order (NLO) running coupling constant α_s has the form:

$$\alpha_s(Q^2) = \frac{12\pi}{(33 - 2n_f) \ln(Q^2/\Lambda_{\overline{MS}}^2)} \left(1 - 6 \frac{153 - 19n_f}{(33 - 2n_f)^2} \frac{\ln(\ln(Q^2/\Lambda_{\overline{MS}}^2))}{\ln(Q^2/\Lambda_{\overline{MS}}^2)} \right). \quad (5)$$

In order to match with the adopted gluon distributions, we choose the same running coupling constant for the hard subprocess and for the gluon distributions. The running behaviors for the above mentioned three groups’ gluon distributions are slightly different, so when taking these different gluon distributions, it also means taking a different running α_s . The value of $\Lambda_{\overline{MS}}$ varies with the active quark flavor number n_f of the process. Taking $\alpha_s(m_Z^2)$ as an input, and in the condition of $Q^2 < m_b^2$, the three groups CTEQ, GRV and MRS obtain their different values for $\Lambda_{\overline{MS}}$,

$$CTEQ5L : \Lambda_{\overline{MS}}(n_f = 4) = 0.192 \quad (\alpha_s(m_Z^2) = 0.127),$$

$$\begin{aligned}
GRV98L : \quad \Lambda_{\overline{MS}}(n_f = 4) &= 0.175 \quad (\alpha_s(m_Z^2) = 0.125), \\
MSRT2001L : \quad \Lambda_{\overline{MS}}(n_f = 4) &= 0.220 \quad (\alpha_s(m_Z^2) = 0.130).
\end{aligned} \tag{6}$$

When $m_b^2 \leq Q^2 \leq m_t^2$ or $Q^2 \geq m_t^2$, the active quark flavor number n_f will change to 5 or 6 accordingly and it's corresponding leading order $\Lambda_{\overline{MS}}$ can be obtained by using Eq.(4) and by the requirement of the continuum of the running α_s . For the two next to leading order gluon distributions CTEQ3M and CTEQ5M, when $n_f = 4$, the value of $\Lambda_{\overline{MS}}$ are([21],[22]),

$$\begin{aligned}
CTEQ3M : \quad \Lambda_{\overline{MS}}(n_f = 4) &= 0.239 \quad (\alpha_s(m_Z^2) = 0.112), \\
CTEQ5M : \quad \Lambda_{\overline{MS}}(n_f = 4) &= 0.326 \quad (\alpha_s(m_Z^2) = 0.118).
\end{aligned} \tag{7}$$

In the present leading order considerations, the energy scale dependence of the estimates can not be eliminated. Only when the higher order processes are taken into account, one can reduce or eliminate such kind of energy scale dependence, which is out of the range of the paper. In the present paper, we take two characteristic energy scales to study the energy scale dependence in the $B_c(B_c^*)$ meson production processes:

Type A:

$$Q^2 = \bar{s}/4,$$

where \bar{s} is the square of the c.m. energy for the subprocess;

Type B:

$$Q^2 = M_{B_c T}^2 = P_T^2 + M^2,$$

which is the square of the so-called $B_c(B_c^*)$ meson's 'transverse mass'.

In TABLEs II, III, IV, V, the total cross-sections for the hadronic production of $B_c(B_c^*)$ at TEVATRON and at LHC with various Q^2 values are put. When computing the cross-sections the running coupling constant, appearing in the gluon distributions, are taken the same as that in the hard subprocess. In the tables, the results for B_c and B_c^* and their excited states, the energy levels at in $1S$ and $2S$ respectively, are included. Since the mesons $B_c(B_c^*)$ with a small P_T (the transverse momentum) cannot be measured, here when calculating the cross-sections we have imposed a cut on P_T (those with $P_T \geq 5$ GeV are taken into account). Furthermore, because those with a big Y (rapidity) component are mainly in the small P_T region and we have set a cut for the small P_T already, thus the big Y events have also been cut 'away'.

TABLE II: Total cross-section for the hadronic production of $B_c(B_c^*)$ for the TEVATRON and with the characteristic energy scale $Q^2 = \bar{s}/4$. The number in parenthesis shows the Monte Carlo uncertainty in the last digit. The cross sections are expressed in nb.

-	Gluon distributions and the order of running α_s					
	CTEQ3M	CTEQ5M	CTEQ5L	CTEQ5L	GRV98L	MSRT2001L
-	NLO	NLO	NLO	LO	LO	LO
$\sigma_{B_c(1^1S_0)}$	0.456(1)	0.590(1)	0.4137(8)	0.829(1)	0.904(2)	0.908(2)
$\sigma_{B_c^*(1^3S_1)}$	1.153(4)	1.496(5)	1.041(4)	2.083(5)	2.277(8)	2.351(9)
$\sigma_{B_c(2^1S_0)}$	0.1150(2)	0.1489(4)	0.1025(2)	0.2047(5)	0.2247(5)	0.2321(6)
$\sigma_{B_c^*(2^3S_1)}$	0.2777(8)	0.355(1)	0.2445(7)	0.485(1)	0.535(1)	0.557(1)

TABLE III: Total cross-section for the hadronic production of $B_c(B_c^*)$ for the TEVATRON and with the characteristic energy scale $Q^2 = P_T^2 + M^2$. The number in parenthesis shows the Monte Carlo uncertainty in the last digit. The cross sections are expressed in nb.

-	Gluon distributions and the order of running α_s					
	CTEQ3M	CTEQ5M	CTEQ5L	CTEQ5L	GRV98L	MSRT2001L
-	NLO	NLO	NLO	LO	LO	LO
$\sigma_{B_c(1^1S_0)}$	0.632(1)	0.844(2)	0.567(1)	1.187(2)	1.258(4)	1.344(4)
$\sigma_{B_c^*(1^3S_1)}$	1.605(5)	2.158(7)	1.455(5)	3.01(1)	3.19(1)	3.40(1)
$\sigma_{B_c(2^1S_0)}$	0.1607(4)	0.2133(5)	0.1429(3)	0.2597(7)	0.3133(8)	0.3370(8)
$\sigma_{B_c^*(2^3S_1)}$	0.392(1)	0.523(1)	0.347(1)	0.717(2)	0.754(2)	0.818(2)

From TABLES II, III, IV, V, one may see that the total hadronic cross section of $B_c(B_c^*)$ meson with the same cut for small P_T (5 GeV) at LHC is almost one order bigger than that of $B_c(B_c^*)$ meson at TEVATRON. This is mainly due to the fact that the collide energy in LHC is much bigger than that of TEVATRON so at LHC more small x partons can give substantial contributions to the total cross sections. From the following figures on P_T distributions one can see that the $B_c(B_c^*)$ transverse momentum P_T distributions at LHC are smoother than the corresponding P_T distributions at TEVATRON. In order to see this

TABLE IV: Total cross-section for the hadronic production of $B_c(B_c^*)$ for the LHC and with the characteristic energy scale $Q^2 = \bar{s}/4$. The number in parenthesis shows the Monte Carlo uncertainty in the last digit. The cross sections are expressed in nb.

-	Gluon distributions and the order of running α_s					
	CTEQ3M	CTEQ5M	CTEQ5L	CTEQ5L	GRV98L	MSRT2001L
-	NLO	NLO	NLO	LO	LO	LO
$\sigma_{B_c(1^1S_0)}$	5.96(1)	8.10(2)	7.93(2)	15.81(4)	17.23(4)	15.52(3)
$\sigma_{B_c^*(1^3S_1)}$	15.31(6)	20.76(8)	20.02(8)	39.4(1)	43.7(1)	38.9(1)
$\sigma_{B_c(2^1S_0)}$	1.561(4)	2.081(6)	2.081(6)	3.97(1)	4.43(1)	3.96(1)
$\sigma_{B_c^*(2^3S_1)}$	3.80(1)	5.22(1)	5.22(1)	9.80(3)	10.89(4)	9.65(3)

TABLE V: Total cross-section for the hadronic production of $B_c(B_c^*)$ for the LHC and with the characteristic energy scale $Q^2 = P_T^2 + M^2$. The number in parenthesis shows the Monte Carlo uncertainty in the last digit. The cross sections are expressed in nb.

-	Gluon distributions and the order of running α_s					
	CTEQ3M	CTEQ5M	CTEQ5L	CTEQ5L	GRV98L	MSRT2001L
-	NLO	NLO	NLO	LO	LO	LO
$\sigma_{B_c(1^1S_0)}$	7.62(2)	10.55(3)	10.05(3)	20.96(5)	22.39(7)	20.32(6)
$\sigma_{B_c^*(1^3S_1)}$	19.60(7)	27.2(1)	26.0(1)	53.8(2)	57.2(2)	51.7(2)
$\sigma_{B_c(2^1S_0)}$	2.010(6)	2.793(8)	2.617(7)	5.39(1)	5.75(1)	5.27(1)
$\sigma_{B_c^*(2^3S_1)}$	4.93(1)	6.88(2)	6.55(2)	13.25(4)	14.12(5)	12.98(4)

factor more clearly, in TABLE VI we list the ratio $\left(\frac{\sigma_{TeV}}{\sigma_{LHC}}\right)_{P_{Tcut}}$, which is the ratio of the cross sections at TEVATRON and at LHC. It change with P_T cuts. Considering the luminosity at LHC is about two order bigger than that at TEVATRON, the B_c events obtained per year at LHC are expected so higher than those at TEVATRON by $3 \sim 4$ order.

From TABLES II, III, IV, V, one may see that the gluon distributions, the running coupling constant and the corresponding energy scale used both in the gluon distribution functions and in the running coupling constant, all affect the total cross sections to a certain

TABLE VI: The relation between the ratio $\left(\frac{\sigma_{Teva}}{\sigma_{LHC}}\right)$ and the $B_c(B_c^*)$ transverse momentum P_T cut P_{Tcut} . The characteristic energy scale is $Q^2 = \bar{s}/4$, the running α_s is in leading order and the gluon distribution is CTEQ5L.

-	B_c				B_c^*			
$P_{Tcut}(GeV)$	0	5	50	100	0	5	50	100
$\left(\frac{\sigma_{Teva}}{\sigma_{LHC}}\right)_{P_{Tcut}} (\times 10^{-2})$	6.26	5.24	1.00	0.31	6.09	5.19	0.97	0.24

degree. For all the three types of leading order gluon distributions CTEQ5L, GRV98L and MSRT2001L, the differences of the corresponding total cross sections are small (about 10%–20%). But the difference caused by using the leading order gluon distribution CTEQ5L and the next to leading order gluon distribution CTEQ3M and CTEQ5M is big (here to be self-consistent, for the leading order gluon distributions we choose the leading order running α_s and for the next to leading order gluon distribution we choose the next to leading order running α_s): at TEVATRON the total cross section for CTEQ5L is about two times as large as that of CTEQ3M and CTEQ5M, while at LHC the total cross section for CTEQ5L is almost 3 times bigger than that of CTEQ3M and CTEQ5M. For the leading order gluon distributions CTEQ5L, GRV98L and MSRT2001L, one may see clearly that the cross sections at TEVATRON and at LHC obtained by the different gluon distributions are quite different: at TEVATRON the cross section corresponding to MSRT2001L is the biggest, while at LHC the biggest one is corresponding to GRV98L.

From TABLEs II, III, IV, V, one may see that the hadronic production cross sections of $B_c(B_c^*)$ meson at $1S$ -level is about $3 \sim 4$ times as large as those of the excited states at $2S$ -level (corresponding to the same spin). This is mainly caused by the parameters relevant to potential model, for example, $f_{B_c(1S)}^2 = 2.25f_{B_c(2S)}^2$. For the same energy level (nS), as expected by spin counting, the vector cross sections are approximately three times as large as the pseudo-scalar cross sections.

In order to show the uncertainties quantitatively for the hadronic production of $B_c(B_c^*)$ at TEVATRON and at LHC, we draw the related differential distributions in transverse momentum P_T and rapidity Y by means of the $B_c(B_c^*)$ generator BCVEGPY. Since the

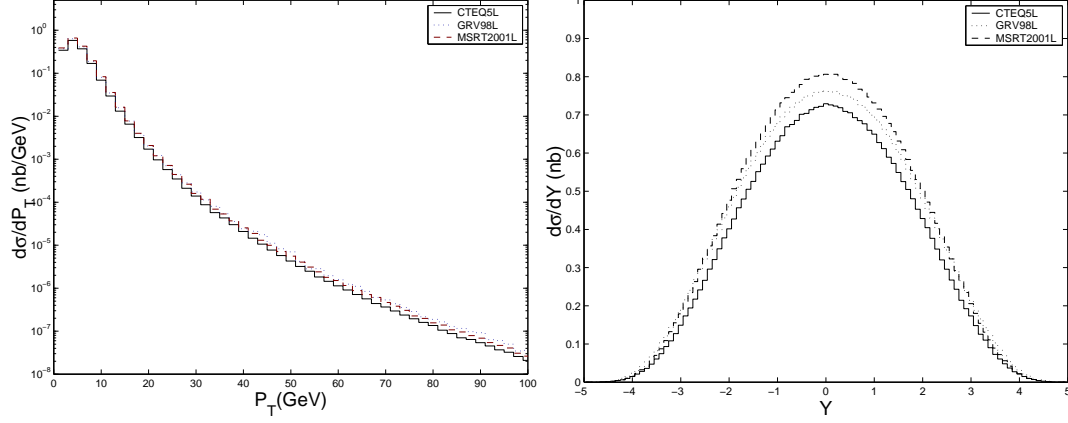


FIG. 6: At TEVATRON, the differential distributions in B_c transverse momentum P_T and rapidity Y for the different leading order gluon distributions CTEQ5L, GRV98L, MSRT2001L. The characteristic energy scale $Q^2 = \bar{s}/4$ and the running α_s is in leading order. The solid line stands for CTEQ5L, dotted line for GRV98L and the dashed line for MSRT2001L.

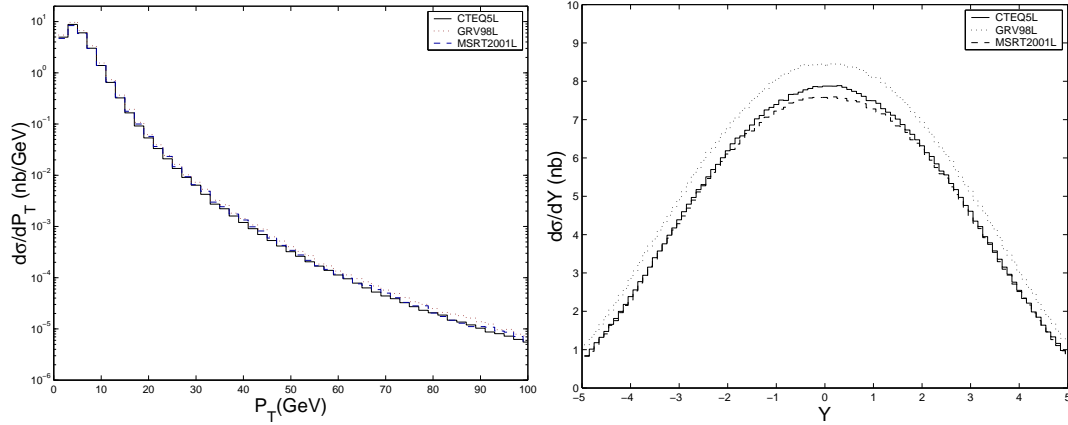


FIG. 7: At LHC, the differential distributions in B_c transverse momentum P_T and rapidity Y for the different leading order gluon distributions CTEQ5L, GRV98L, MSRT2001L. The characteristic energy scale $Q^2 = \bar{s}/4$ and the running α_s is in leading order. The solid line stands for CTEQ5L, dotted line for GRV98L and the dashed line for MSRT2001L.

behavior for B_c and B_c^* are very similar, so here to study the uncertainties emphasized in this subsection, we compute and show the P_T and Y distributions for the pseudo-scalar B_c meson only. Without specific statements, we will take the leading order gluon distribution CTEQ5L, leading order running α_s and Type A energy scale as basic input.

The dependence of the differential distributions on B_c transverse momentum P_T and

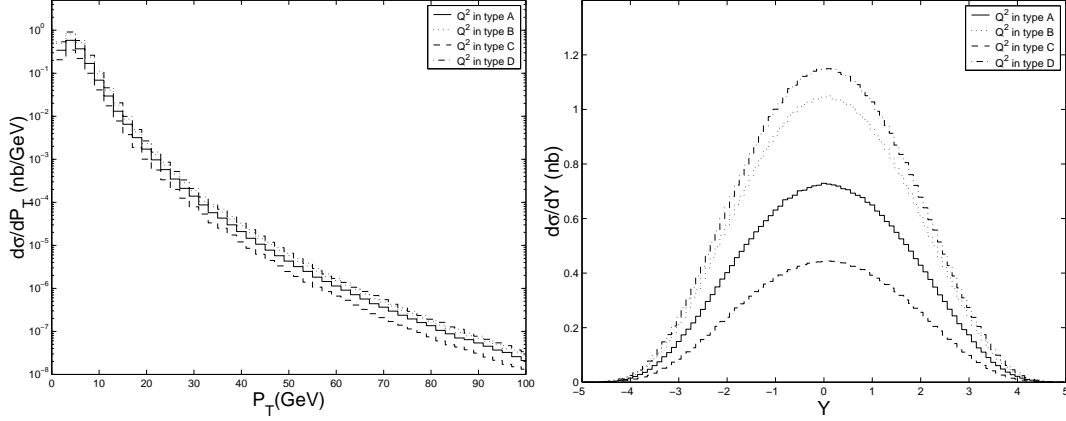


FIG. 8: At TEVATRON, the differential distributions in B_c transverse momentum P_T and rapidity Y for the four types of the characteristic energy scale. The gluon distribution is chosen as CTEQ5L and the running α_s is in leading order. The solid line stands for type A, the dotted line stands for type B, the dashed line for type C and the dash-dot line for type D.

rapidity Y at TEVATRON and at LHC are computed with the gluon distributions CTEQ5L, GRV98L and MSRT2001L (leading order ones) and are put in FIGs.6,7. When doing the computation, the characteristic energy scale is fixed to Type A, i.e., $Q^2 = \bar{s}/4$ and the running α_s is in leading order. From FIGs. 6,7, one may see that the differential distributions in P_T and Y are very similar (in FIGs.6,7 the differential distributions in P_T and Y are denoted by the logarithmic coordinate and the linear coordinate, respectively) corresponding to the three gluon distributions. From the figures the relative difference is visible among the obtained differential distributions in P_T and Y of the production at TEVATRON and at LHC with the three gluon distributions CTEQ5L, GRV98L and MSRT2001L respectively, although some of the difference has already been shown in TABLEs II, III, IV, V. At TEVATRON, the distributions for the MSRT2001L are the largest, followed by the GRV98L and then the CTEQ5L; while at LHC, the distributions for the GRV98L are the largest, followed by CTEQ5L and then the MSRT2001L.

In FIGs.8,9, the differential distributions in B_c transverse momentum P_T and rapidity Y at TEVATRON and at LHC for the four types of the characteristic energy scale are presented. Here the gluon distributions are chosen to be CTEQ5L and the running α_s is in leading order. In order to show the scale dependence more, in addition to the two ways to fix the energy scale as stated above: Type A and Type B, we take two more: Type C and

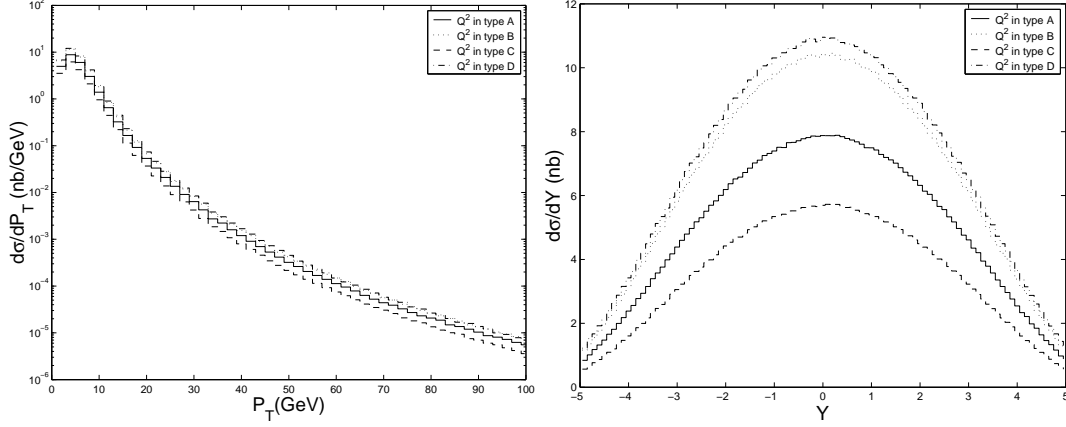


FIG. 9: At LHC, the differential distributions in B_c transverse momentum P_T and rapidity Y for the four types of the characteristic energy scale. The gluon distribution is chosen as CTEQ5L and the running α_s is in leading order. The solid line stands for type A, the dotted line stands for type B, the dashed line for type C and the dash-dot line for type D.

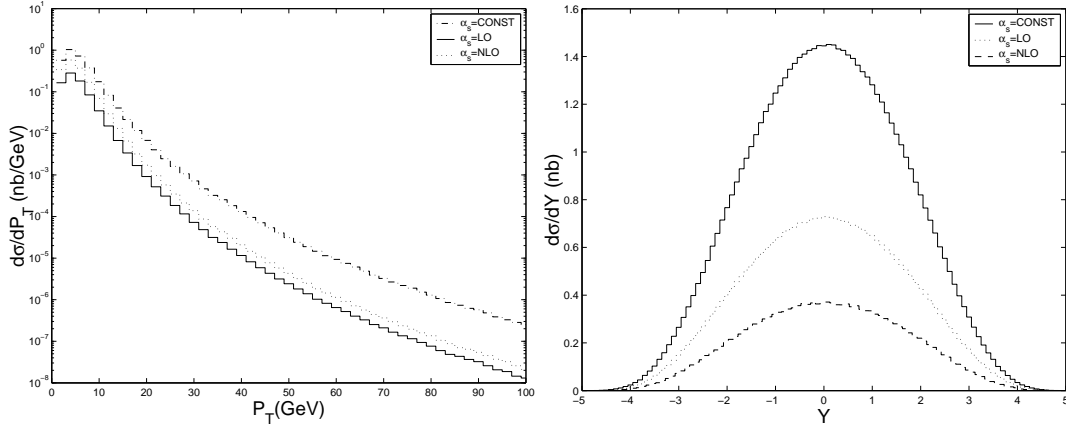


FIG. 10: At TEVATRON, the differential distributions in B_c transverse momentum P_T and rapidity Y for the different order of running α_s . The gluon distribution is chosen as CTEQ5L and the characteristic energy scale is in type A, i.e. $Q^2 = \bar{s}/4$. The solid line stands for leading order running α_s , the dotted line for next to leading order running α_s and the dash-dot line for constant $\alpha_s = 0.22$.

Type D into our study. For Type C, $Q^2 = \bar{s}$, where \bar{s} is the square of the c.m. energy for the subprocess; for Type D, $Q^2 = p_{Tb}^2 + m_b^2$, and $Q^2 = p_{Tb}^2 + m_b^2$ is the square of the b quark transverse mass.

All the obtained total hadronic production cross sections and the different differential

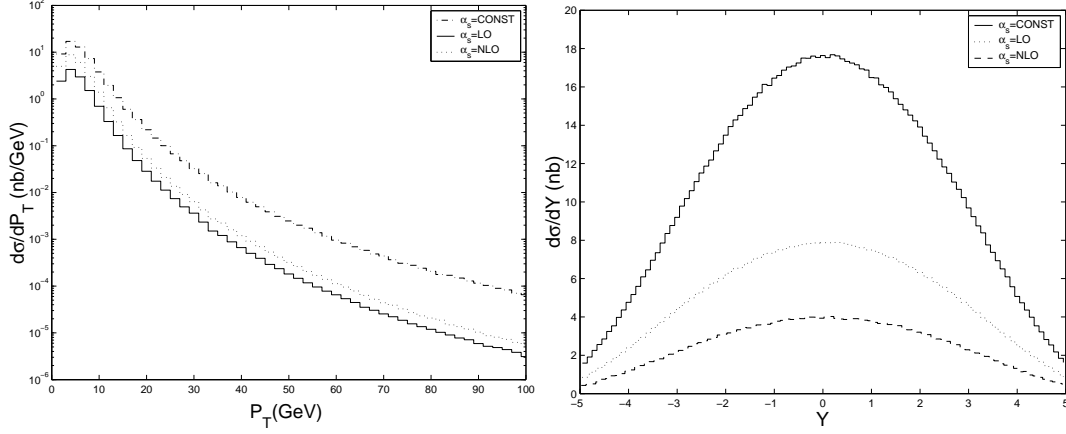


FIG. 11: At LHC, the differential distributions in B_c transverse momentum P_T and rapidity Y for the different order of running α_s . The gluon distribution is chosen as CTEQ5L and the characteristic energy scale is in type A, i.e. $Q^2 = \bar{s}/4$. The solid line stands for leading order running α_s , the dotted line for next to leading order running α_s and the dash-dot line for constant $\alpha_s = 0.22$.

distributions here are computed by using the $B_c(B_c^*)$ generator BCVEGPY, which is programmed under the lowest gluon-gluon fusion process $gg \rightarrow B_c(B_c^*) + b + \bar{c}$. Since a complete pQCD calculation on the production to the next order is too complicated, to have some ideas on the higher order contributions (corrections), as done by some authors in literature we take two ways to see some higher order corrections: one is to take the next leading order gluon distributions and with next leading order running α_s , and the other is to take the next leading order running α_s but with the leading order gluon distribution. The first way is done by choosing the next leading order gluon distributions as CTEQ3M and CTEQ5M, and the results (cross-sections only) have been put in TABLEs II, III, IV, V. As for the second way, we take CTEQ5L as the representation of the leading order gluon distributions, the differential distributions in B_c transverse momentum P_T and rapidity Y at TEVATRON and at LHC for the different order of running α_s are computed and put in FIGs.10,11, where α_s has several choices and the characteristic energy scale is chosen to be type A, i.e., $Q^2 = \bar{s}/4$. For comparison, in FIGs.10,11, the results for a constant $\alpha_s = 0.22$ have also been included.

Finally, in order to show the relative magnitude for the theoretical uncertainties of B_c meson production caused by the different gluon distributions, the different characteristic

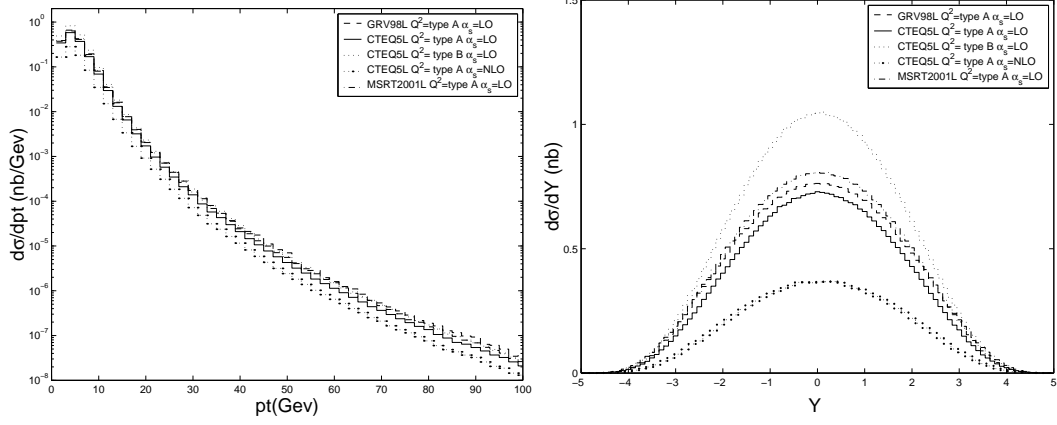


FIG. 12: At TEVATRON, the differential distributions in B_c transverse momentum P_T and rapidity Y for different gluon distributions, different characteristic energy scale and different order of running α_s .

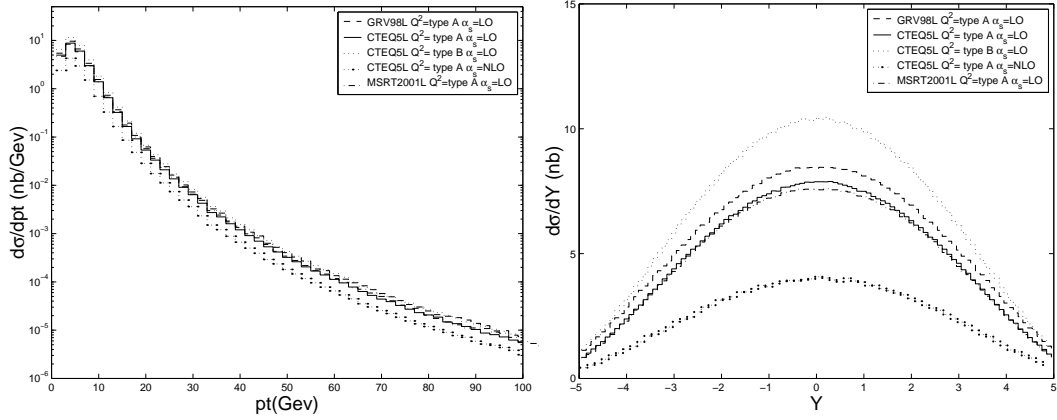


FIG. 13: At LHC, the differential distributions in B_c transverse momentum P_T and rapidity Y for different gluon distributions, different characteristic energy scales and different order of running α_s .

energy scales and the different order of running α_s , in FIGs. 12,13, we present the differential distributions in B_c transverse momentum P_T and rapidity Y at TEVATRON and at LHC for different gluon distributions, different characteristic energy scale and different order of running α_s . In the figures the dashed line and the dash-dot line stand for the gluon distributions GRV98L and MSRT2001L respectively with Q^2 of Type A and the running α_s in leading order. The solid line stands for Q^2 in type A and the running α_s in leading order; the dotted line for Q^2 in type B and the running α_s in leading order; the dotted line

with full dots for Q^2 in type A and the running α_s in next to leading order, while all of the solid line, the dotted line and the dotted line with full dots stands for the gluon distributions CTEQ5L. From FIGs. 12,13, one may see that of the present considered leading order factors, the characteristic energy scale is the most sensitive one in the hadronic production of B_c meson.

III. KINEMATIC CUTS FOR THE $B_c(B_c^*)$ MESON HADRONIC PRODUCTION

Experimentally, considering the abilities of detectors, only the produced events in a certain kinematic region, can be observed e.g. for the $B_c(B_c^*)$ meson production at a hadronic collider, an event with a small transverse momentum P_T or a large rapidity Y of the produced $B_c(B_c^*)$ meson can not be directly detected by the detectors and thus it can not be utilized for the studies, because the detector cannot cover the direction along the beam and the produced B_c meson in the event moves very close to the beam direction. Therefore to consider the ‘useful’ events in the estimates, the kinematic cuts on P_T and Y of the produced $B_c(B_c^*)$ meson can not be avoided. For experimental useful reference, the values of the cuts should dictate the detector’s abilities. In this section we try some possible values for these kinematic cuts and then compute and present the corresponding differential distributions precisely.

First we study the differential distributions for the $B_c(B_c^*)$ meson production at TEVATRON and at LHC with the different $B_c(B_c^*)$ rapidity cuts Y_{cut} (here for a precise value of Y_{cut} , we mean that the events only with $|Y| \leq Y_{cut}$ are taken into account, here Y is the rapidity of the B_c meson). At TEVATRON (CDF, D0 and BTeV) the rapidity cut Y_{cut} experimentally roughly is about 1.5, and at LHC due to a higher rapidity resolution (ATLAS, CMS and LHC-B), the value of Y_{cut} may be higher. Therefore consider the range of the detectors, we choose five different Y_{cut} , i.e., $Y_{cut} = (0.5, 1.0, 1.5, 2.0, 2.5)$ to compute the observables. Moreover, since the uncertainties have already been studied quantitatively in the last section, such as those come from various versions of the parton distribution functions by various groups, the variation of the parameters in the estimates relevant to the potential model, α_s -running, the characteristic energy scale of the process etc, so here we present the results only for the one choice for the uncertainties with CTEQ5L for gluon distribution, the leading order running α_s and type A characteristic energy scale ($Q^2 = \bar{s}^2/4$).

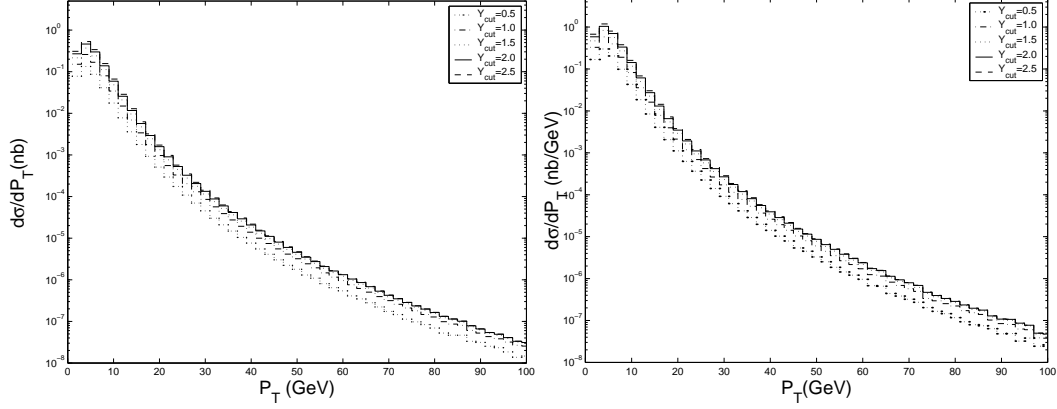


FIG. 14: At TEVATRON, the differential distributions in pseudo-scalar B_c meson P_T (left diagram) and in vector B_c^* meson P_T (right diagram) with various Y_{cut} . The dashed line stands for $Y_{cut} = 2.5$, the solid line for $Y_{cut} = 2.0$, the dotted line for $Y_{cut} = 1.5$, the dash-dot line for $Y_{cut} = 1.0$ and the dotted line with big dots for $Y_{cut} = 0.5$.

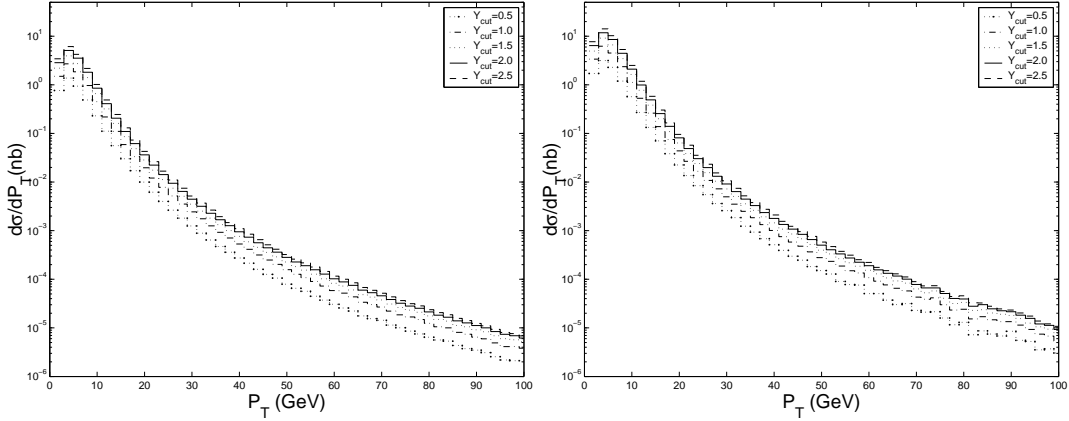


FIG. 15: At LHC, the differential distributions in pseudo-scalar B_c meson P_T (left diagram) and in vector B_c^* meson P_T (right diagram) with various Y_{cut} . The dashed line stands for $Y_{cut} = 2.5$, the solid line for $Y_{cut} = 2.0$, the dotted line for $Y_{cut} = 1.5$, the dash-dot line for $Y_{cut} = 1.0$ and the dotted line with big dots for $Y_{cut} = 0.5$.

From the differential distributions of the produced B_c shown in FIGs.14,15, one may see the differential distributions varying with Y_{cut} and P_{Tcut} . The dependence can be seen more explicitly in FIG. 14 than in FIG. 15, because at TEVATRON the rapidity distribution is smaller than the rapidity distribution at LHC, and then the rapidity cut's influence to the detection at LHC will be greater. The differential distributions varying with Y_{cut} will

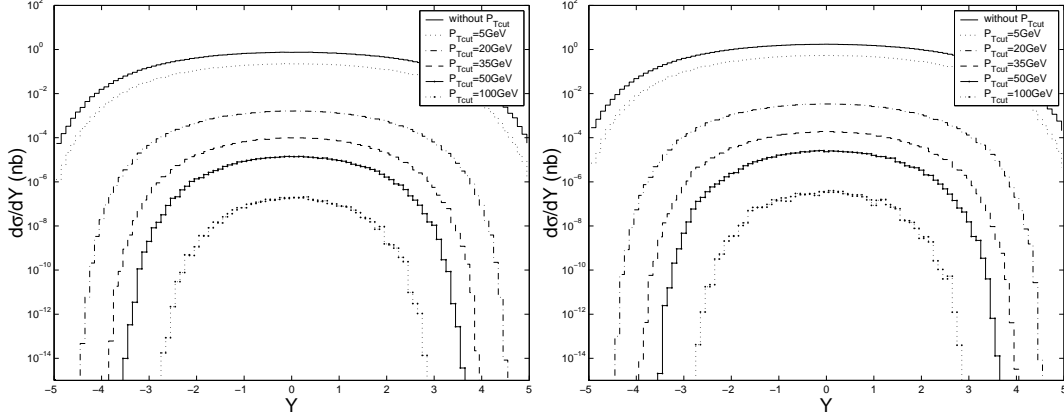


FIG. 16: At TEVATRON, the differential distributions in pseudo-scalar B_c meson Y (left diagram) and in vector B_c^* meson Y (right diagram) with various P_{Tcut} . The solid line stands for the full production without P_{Tcut} , the dashed line for $P_{Tcut} = 5.0\text{GeV}$, the dash-dot line for $P_{Tcut} = 20.0\text{GeV}$, the dotted line for $P_{Tcut} = 35.0\text{GeV}$ and the solid line with big dots for $P_{Tcut} = 50.0\text{GeV}$ and the dashed line with big dots for P_{Tcut} .

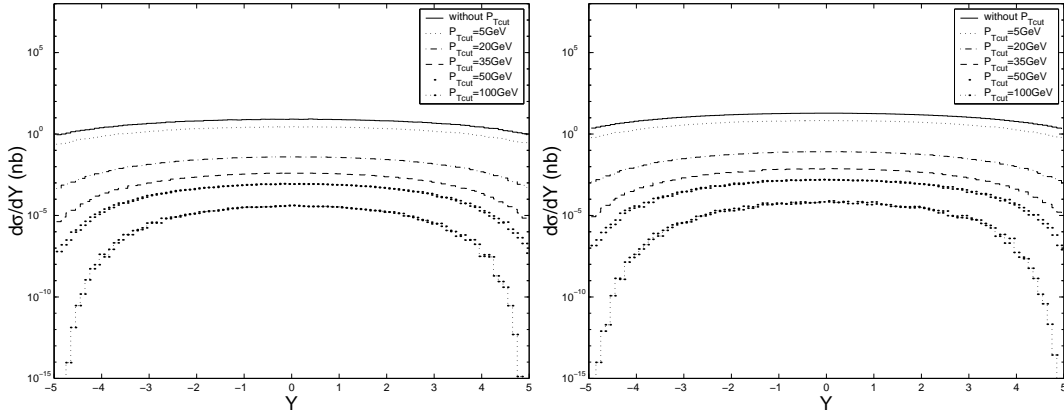


FIG. 17: At LHC, the differential distributions in pseudo-scalar B_c meson Y (left diagram) and in vector B_c^* meson Y (right diagram) with various P_{Tcut} . The solid line stands for the full production without P_{Tcut} , the dashed line for $P_{Tcut} = 5.0\text{GeV}$, the dash-dot line for $P_{Tcut} = 20.0\text{GeV}$, the dotted line for $P_{Tcut} = 35.0\text{GeV}$ and the big dotted line for $P_{Tcut} = 50.0\text{GeV}$ and the dashed line with big dots for P_{Tcut} .

decrease with the increment of P_T , this is mainly due to the fact that with the increment of P_T , the dependence of the differential distributions on the rapidity Y becomes smaller and smaller, and then the rapidity cut Y_{cut} becomes less important, thus when the value of P_T

TABLE VII: At TEVATRON, the ratio $R_{P_{Tcut}}$ for the pseudo-scalar B_c and the vector B_c^* . (The definition about $R_{P_{Tcut}}$ is in text)

P_{Tcut}		0GeV			5GeV			20GeV			35GeV			50GeV		
Y_{cut}		1.0	1.5	2.0	1.0	1.5	2.0	1.0	1.5	2.0	1.0	1.5	2.0	1.0	1.5	2.0
$R_{P_{Tcut}}$	B_c	0.45	0.64	0.79	0.46	0.65	0.80	0.57	0.77	0.91	0.65	0.85	0.95	0.70	0.90	0.98
	B_c^*	0.45	0.64	0.79	0.46	0.65	0.80	0.57	0.77	0.90	0.64	0.84	0.95	0.70	0.89	0.98

increases to an enough large value, the border of the differential distributions for the rapidity becomes smaller than Y_{cut} and then the differential distribution in P_T with cut is coincide with the differential distribution in P_T without cut. In FIGs. 16,17, one may see the factor more clearly, in which we draw the dependence of the differential distributions on rapidity Y with different P_{Tcut} for the hadronic production of $B_c(B_c^*)$ meson at TEVATRON and at LHC. From FIGs. 16,17, one may see that the dependence of the differential cross sections on rapidity at LHC presents a broader behavior than that at TEVATRON, so the rapidity cut's influence to the LHC is greater. In order to focus on the difference of the differential distributions on the P_{Tcut} and Y_{cut} at TEVATRON and at LHC quantitatively, we introduce the ratio of total hadronic cross sections,

$$R_{P_{Tcut}} = \left(\frac{\sigma_{Y_{cut}}}{\sigma_0} \right)_{P_{Tcut}} \quad (8)$$

where σ_0 is the total hadronic cross section without Y_{cut} and $\sigma_{Y_{cut}}$ is the total hadronic cross section with a cut Y_{cut} . The ratio $R_{P_{Tcut}}$ changes with the cut value of P_{Tcut} , and as is shown in TABLEs VII,VIII, for a fixed Y_{cut} , the value of $R_{P_{Tcut}}$ becomes larger and larger with P_{Tcut} increasing. The reason is that the differential distributions versus the rapidity Y decrease with the increment of P_T in the range, so the contributions to the total hadronic cross section from the part within the cut, i.e. ($|Y| \leq Y_{cut}$), increases with the increment of P_T .

For the $B_c(B_c^*)$ meson production, only at high energy hadronic colliders numerous enough B_c mesons may be produced. It is very clear that the $B_c(B_c^*)$ meson production at hadronic collider is quite sensitive to the c.m. energy of the collider. Concerning that RUN-II is carrying on now at a slight higher energy than that (1.8TeV) for RUN-I for TEVATRON,

TABLE VIII: At LHC, the ratio $R_{P_{Tcut}}$ for the pseudo-scalar B_c and the vector B_c^* . (The definition about $R_{P_{Tcut}}$ is in text)

P_{Tcut}		0GeV			5GeV			20GeV			35GeV			50GeV		
Y_{cut}		1.0	1.5	2.0	1.0	1.5	2.0	1.0	1.5	2.0	1.0	1.5	2.0	1.0	1.5	2.0
$R_{P_{Tcut}}$	B_c	0.31	0.46	0.59	0.32	0.47	0.60	0.38	0.54	0.69	0.42	0.60	0.74	0.45	0.64	0.79
	B_c^*	0.31	0.46	0.59	0.32	0.47	0.60	0.38	0.54	0.69	0.42	0.59	0.74	0.45	0.63	0.78

TABLE IX: The total hadronic cross sections for TEVATRON at different c.m. energies. The gluon distribution is chosen as CTEQ5L and the characteristic energy scale of the production is chosen as type A, i.e. $Q^2 = \bar{s}/4$. In addition, a cut for transverse momentum P_T ($P_T < 5GeV$) and a cut for rapidity Y ($|Y| > 1.5$) have been imposed. Here the number in parenthesis at the end of each value means the Monte Carlo uncertainty of evaluating the phase-space integration in the last digit of the value.

TEVATRON c.m. energy	1.8(TeV)	1.9(TeV)	1.96(TeV)	2.0(TeV)
$B_c[{}^1S_0]$	0.4006(3)	0.4352(3)	0.4562(3)	0.4709(3)
$B_c^*[{}^3S_1]$	1.0031(7)	1.0879(8)	1.1434(8)	1.1784(8)

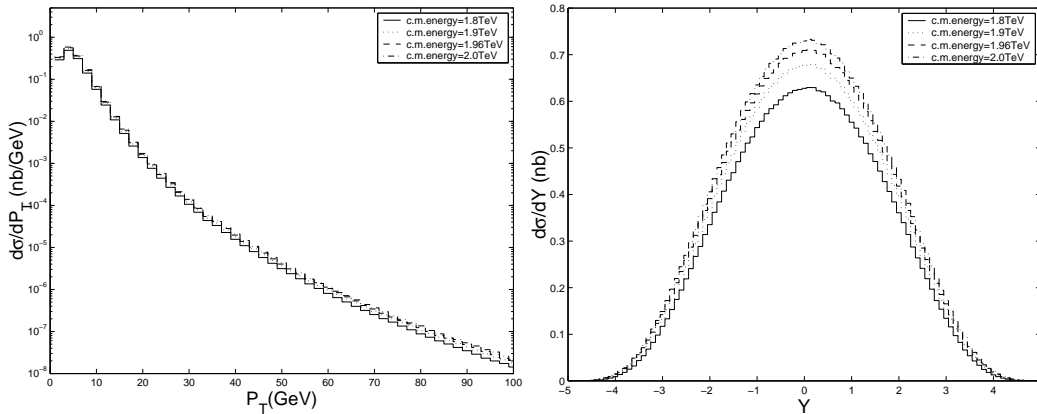


FIG. 18: At TEVATRON, the differential distributions in the B_c transverse momentum P_T and rapidity Y with different TEVATRON c.m. energy. The solid line stands for the case of 1.8TeV, the dotted line for 1.9TeV, the dashed line for 1.96TeV and the dash-dot line for 2.0TeV.

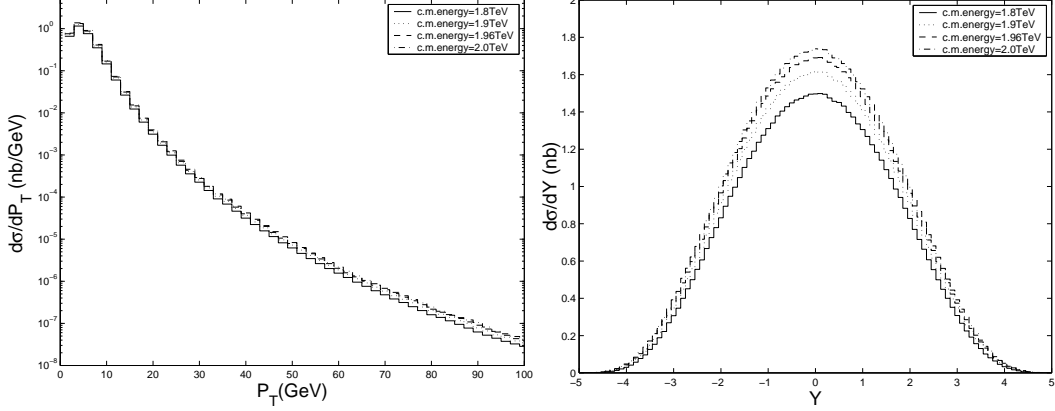


FIG. 19: At TEVATRON, the differential distributions in the B_c^* transverse momentum P_T and rapidity Y with different TEVATRON c.m. energy. The solid line stands for the case of 1.8TeV, the dotted line for 1.9TeV, the dashed line for 1.96TeV and the dash-dot line for 2.0TeV.

we take the TEVATRON for an example to study the differences caused by the slight change of the c.m. energy. Since its c.m. energy is designed to be 2.0TeV, so here we take several typical c.m. energies, i.e., 1.8TeV, 1.9TeV, 1.96TeV and 2.0TeV to compute the B_c production. The results, i.e., the differential distributions for the $B_c(B_c^*)$ transverse momentum P_T and rapidity Y are presented in FIGs.18,19, and total cross-section with suitable cuts are presented in TABLE IX. From the table one may see that roughly speaking when the c.m. energy of TEVATRON increase from 1.8TeV to 2.0TeV, the cross-section increases quite a lot about 20%.

IV. SUMMARY

In this paper, we have studied the uncertainties in estimates of the $B_c(B_c^*)$ -meson hadronic production quantitatively. All those studies are based on the newly completed $B_c(B_c^*)$ generator BCVEGPY. The uncertainties are computed precisely, which come from various versions of the parton distribution functions given by various groups, the variation of the parameters relevant to the potential model, the strong coupling α_s relevant to its running and the characteristic energy scale of the process where the QCD factorization are carried out and etc. Of them we have found the characteristic energy scale of the process where the QCD factorization are carried out is the most. We have also studied the differences at LHC and at TEVATRON for the observables with reasonable various kinematic cuts, especially,

the cuts on $B_c(B_c^*)$ meson transverse momentum P_T and rapidity Y . We also point out that at TEVATRON from RUN-I to RUN-II due to the collision c.m. energy increasing, the cross-section of the B_c production increase about 20% that is quite a lot of increment. Considering the situation that TEVATRON is running and LHC is under constructing, from the results obtained here one may see the fact clearly that the experimental B_c studies at TEVATRON and at LHC are complimentary and simulative.

Acknowledgement The authors would like to thank Yu-Qi Chen and Guo-Ming Chen for discussions, and to thank Vaia Papadimitriou for the suggestion to compute the production at various c.m. energies for TEVATRON. This work was support in part by Nature Science Foundation of China (NSFC).

-
- [1] CDF Collaboraten, F. Abe, *et al.*, Phys. Rev. **D58**, 112004 (1998).
 - [2] K. Anikeev, *et al.*, hep-ph/0201071.
 - [3] Chao-Hsi Chang, *Proceedings of the XXXVIIIth RENCONITRES DE MORIOND* Les Arcs, Savoie, France, **2002 QCD and High Energy Hadronic Interactions**, p-27, hep-ph/20205112.
 - [4] C. Quigg, *Proceedings of the Workshop on B Physics at Hadron Accelerators*, Snowmass (CO) USA, 1993, Eds. P. McBride and C.S. Mishra.
 - [5] Chao-Hsi Chang and Yu-Qi Chen, Phys. Rev. D **46**, 3854 (1992); Erratum Phys. Rev. **50**, 6013 (1994).
 - [6] E. Braaten, K. Cheung and T.C. Yuan, Phys. Rev. D **48**, 4230 (1993); E. Braaten, K. Cheung and T.C. Yuan, Phys. Rev. D **48**, R5049 (1993).
 - [7] Chao-Hsi Chang and Yu-Qi Chen, Phys. Rev. D **48**, 4086 (1993).
 - [8] Chao-Hsi Chang, Yu-Qi Chen, Guo-Ping Han and Hung-Tao Jiang, Phys. Lett. B **364**, 78 (1995); Chao-Hsi Chang, Yu-Qi Chen and R. J. Oakes, Phys. Rev. D **54**, 4344 (1996); K. Kolodziej, A. Leike and R. Rückl, Phys. Lett. B **355**, 337 (1995).
 - [9] A.V. Berezhnoy, V.V. Kiselev, A.K. Likhoded, Z. Phys. A **356**, 79 (1996); S.P. Baranov, Phys.

- Rev. D **56** 3046, (1997).
- [10] K. Cheung, Phys. Lett. B **472**, 408 (2000).
 - [11] Yu-Qi Chen and Yu-Ping Kuang, Phys. Rev. D **46**, 1165 (1992); E. Eichten, C. Quigg, Phys. Rev. D **49** 5845 (1994); Phys. Rev. D **52**, 1726 (1995); S.S. Gershtein, V.V. Kiselev, A.K. Likhoded and A.V. Tkabladze, Phys. Rev. D **51**, 3613 (1995).
 - [12] Chao-Hsi Chang, Yu-Qi Chen, Phys. Rev. **D49**, 3399 (1994); Chao-Hsi Chang and Yu-Qi Chen, Commun. Theor. Phys. **23** (1995) 451.
 - [13] A. Abd El-Hady, J.H. Munoz and J.P. Vary; Phys. Rev. **D62** 014014 (2000).
 - [14] N. Isgur, D. Scora, B. Grinstein and M. Wise, Phys. Rev. D **39**, 799 (1989); M. Lusignoli and M. Masetti, Z. Phys. C **51**, 549 (1991); D. Scora and N. Isgur, Phys. Rev. D **52**, 2783 (1995). Dongsheng Du, G.-R. Lu and Y.-D. Yang, Phys. Lett. B **387**, 187 (1996); Dongsheng Du, *et al.*, Phys. Lett. B **414**, 130(1997); Jia-Fu Liu and Kuang-Ta Chao, Phys. Rev. D **56** 4133, (1997); P. Colangelo and F.De Fazio, Phys. Rev. D **61** 034012 (2000). V.V. Kiselev, A.E. Kovalsky and A.K. Likhoded, Nucl. Phys. B **585** 353 (2000); V.V. Kiselev, A.K. Likhoded and A.I. Onishchenko, Nucl. Phys. B **569** 473, (2000). M.A. Nobes and R.M. Woloshyn, J. Phys. G **26** 1079, (2001).
 - [15] Chao-Hsi Chang, Shao-Long Chen, Tai-Fu Feng and Xue-Qian Li, Phys. Rev. D **64**, 014003 (2001); Commun. Theor. Phys. **35**, 51 (2001).
 - [16] M. Beneke and G. Buchalla, Phys. Rev. D **53**, 4991 (1996).
 - [17] Chao-Hsi Chang, J.-P. Cheng and C.-D. Lü, Phys. Lett. **B 425**, 166 (1998); P. Colangelo and F. De Fazio, Mod. Phys. Lett. **A 14**, 2303 (1999); Chao-Hsi Chang, Cai-Dian Lü, Guo-Li Wang and Hong-Shi Zong, Phys. Rev. **D60** 114013, 1999; Chao-Hsi Chang, Yu-Qi Chen, Guo-Li Wang and Hong-Shi Zong, Phys. Rev. D **65**, 014017 (2001); Commun. Theor. Phys. **35**, 395 (2001); Chao-Hsi Chang, Anjan K. Giri, Rukmani Mohanta and Guo-Li Wang, J. Phys. G **28**, 1403, (2002), hep-ph/0204279; Xing-Gang Wu, Chao-Hsi Chang, Yu-Qi Chen and Zheng-Yun Fang, Phys. Rev. D, **67**, 0704XX, (2003), hep-ph/0209125.
 - [18] Chao-Hsi Chang, Chafik Driouich, Paula Eerola and Xing-Gang Wu, hep-ph/0309120.
 - [19] T. Sjostrand, Comput. Phys. Commun. **82** (1994) 74.
 - [20] A.V. Berezhnoy, V.V. Kiselev, A.K. Likhoded and A.I. Onishchenko, Phys. Atom. Nucl. **60**, 1729 (1997); hep-ph/9703341;
 - [21] H.L.Lai, *etal.*, Eur.Phys.J.**C12**, 375(2000)

- [22] H.L.Lai, et al., Preprint MSU-HEP/41024;
- [23] M.Glueck, E.Reya, A.Vogt, Eur.Phys.J.**C5**, 461(1998);
- [24] A.D.Martin, R.G.Roberts, W.J.Stirling and R.S.Thorne, Eur.Phys.J.**C23**, 73(2002);
- [25] Based on the potential model point of view, B_c is the ground state of $(c\bar{b})$ binding-system in 1S_0 and B_c^* is that in 3S_1 .
- [26] At high energy hadronic colliders, numerous B_c may be produced and furthermore the meson B_c has very large branching ratio to decay to B_s meson, $Br(B_c \rightarrow B_s \cdots) \simeq$ several tens percents[12, 13, 14], so the B_s mesons obtained by such B_c decays are tagged precisely at B_c decay vertex, as long as the charge of the meson B_c and/or its decay products is detected. The meson B_s at its production position being tagged has great advantages in the studies of the meson B_s in hadronic environment[3, 4], so at TEVATRON, especially, at LHC the studies of B_s meson in such a way are interesting greatly.
- [27] According to non-relativistic QCD (NRQCD), though there may be non-color-singlet components for physical B_c meson, in contrary J/ψ in the case of hidden flavor (B_c in flavors explicit), with such small components one cannot find a subprocess in an order lower in pQCD for B_c hadronic production as in the case of J/ψ production. Therefore the subprocess is dominant for sure.
- [28] www address:<http://durpdg.dur.ac.uk/hepdata/pdf>